Directivity of a simplified aeroengine

Pierre-Olivier Mattei

To cite this version:

Pierre-Olivier Mattei. Directivity of a simplified aeroengine. Acta Acustica united with Acustica, 2006, 92 (2), pp.225-235. hal-00089053

HAL Id: hal-00089053
https://hal.science/hal-00089053

Submitted on 15 Jan 2008

Directivity of a simplified aeroengine

P.-O. Mattei

Laboratoire de Mécanique et d'Acoustique

31 chemin Joseph Aiguier

13402 Marseille cedex 20 (France)

(29 pages, 16 figures)

Summary

This paper presents theoretical and numerical results on the high frequency directivity of an aeroengine under flight conditions. In this paper, two different theories, based on a Kirchhoff approximation for semi-infinite cylinders, are combined to obtain the far field sound pressure radiated into the whole surrounding space. Although the geometric description of the engine is simplified - in particular, the annular exhaust is not taken into account - it includes some of the main features of a typical aeroengine: subsonic flow, different diameters at the intake and the exhaust ends and the occurence of various flow velocities at the exhaust end to account for the effects of a jet. Numerical examples are given.

PACS no. 43.20.El, 43.28.Py, 43.50.Lj, 43.50.Nm

1 Introduction

The sound radiation emitted by aeroengines has been studied for a long time. From the first studies [5, 18, 17, 12] on the acoustic transmission in a pipe with flow, to those dealing with more complex complex such as those focusing on more realistic aeronautical engines (see for example [22, 21, 20, 19, 23, 16]), this topic has attracted considerable attention. Schematically, the studies published so far have been of two kinds. Those of the the first kind have focused on the ends of the engine (the intake and exhaust points) using analytical methods. Those of the second kind have attempted to provide a more realistic description of the engine in numerical terms (mainly using boundary element methods). In the latter studies, however, the description of the engine has always been oversimplified, especially as far as the geometry is concerned; the problem generally treated has been that of a finite cylindrical shell immersed in a uniform flow. To the author's knowledge, the problem of an aeroengine with various diameters at the intake and exhaust points in the presence of a jet has never been addresses so far. When addressing such complex problem, it would obviously be unrealistic to attempt to account completely for the geometry in terms of simple analytical relations. But if some approximations are made, such as neglecting the interferences between the sound pressure fields created by each end of the engine, or assuming that exhaust jet is always circular, it is possible, by combining the results of the previous studies, to obtain a simple asymptotic expression with which the far field sound radiation emitted by an aeroengine can be readily calculated.

This paper deals with the propagation of high frequency sound radiated by an aeroengine without annular exhaust jet under flight conditions. The approach used here is based on theories previously developed by Cargill [3] and by Candel and Homicz & Lordi [2, 11]. This engine is immersed in a uniform subsonic flow and is prolonged by a jet in which the Mach number differs from the external Mach number. The engine is assumed to form a thin finite cylindrical surface. This cylinder is composed of two sections with different diameters that radiate the sound pressure independently. To deal with the acoustic pressure propagating inside each section of the engine, each section is assumed to constitute an infinite semi cylinder. This assumption is based on the idea that the various blade rows of the engine divide the initial finite domain into two independent domains in which the sound pressure field propagates toward the outet end of the two sub domains independently. The acoustic field propagating in each section is therefore only an outgoing field and the acoustic pressure field reflected by the core of the aeroengine is negligible. The acoustic radiation emitted at the aperture of each cylinders is described by the Kirchhoff's approximation. The radiation is taken here to depend only on the field at the open end of each cylinder, neglecting the interferences radiated between the fields by engine's intake and exhaust and by the diffraction from the walls of the cylinder itself. This latter approximation obviously falsifies the results obtained on the rear arc of each cylinder, but this portion of space is that where the radiation emitted by the other part of the engine excited by the same sources becomes prevalent. An other approximation of this model is that the exit plane field of each cylinder is determined by assuming that at sufficiently high frequencies (above the cut-off frequency of the incident propagating mode) no reflection will occur at the exit plane and the pressure field at this point will therefore be that of the incident mode. With this model, one obviously cannot describe duct modes near the cut-off as they radiate at an angle of almost 90^o and have a strong reflection coefficient at the termination. But as established by Cargill [4] upon studying the analytical solution obtained using a Wiener-Hopf approach to the low frequency radiation of an incident plane wave in a pipe with different internal and external flows and by Rienstra [20] upon studying the acoustic radiation occuring in an annular duct in a uniform flow, the reflection coefficient of the plane wave and low modal order waves decreases rapidly to zero as the frequency increases. This is not a crucial point for practical applications since the high frequency contribution to the far field is masked by the other modes. It is also worth noting that Rienstra's solution, while not taking the presence of a primary exhaust jet into account, makes the problem of high by-pass ratio easier to handle.

A similar approach was recently developed by Joseph et al. [14], who modelled the sound radiation of the semi-infinite cylinder using a Wiener-Hopf approximation [13, 15]: this model is valid at low frequencies but does not take the effects of a jet into account.

At the intake end of the engine, the cylinder is taken here to be immersed in a uniform subsonic flow, with the same flow velocity inside and outside the cylinder. The acoustic sound pressure radiated is easily calculated from the directivity diagram for a fluid at rest based on the Prandtl-Glauert transformation [2, 11].

At the exhaust end, the cylinder is immersed in the same flow as the intake end, but inside the cylinder and in an infinitely long circular domain with the same diameter, the internal flow has some characteristics that differ from the external flow, namely the sound speed velocity, density and Mach number. Although the jet emitted by an aeroengine is not circular, it can be reasonably assumed that the acoustic behavior of the exhaust is fairly accurately described by this model on the whole.

The acoustic radiation model chosen here was that proposed by Cargill [3], which is based on a Kirchhoff approximation of the sound radiated from a semi-infinite duct with various internal and external mean flows. Since the results obtained are valid both for a uniform flow and a fluid at rest, this model was also used to compute the sound radiated by the intake of the engine. This model is valid *a priori* only in the case of the front arc of the cylinder (between 0^o and 90^o) and it is a high frequency model: Cargill gives $kR \approx 10$ as the low frequency limit where k is the wavenumber and R the radius of the cylinder. However, comparisons between the results obtained using this method in homogeneous fluid at rest and those obtained with an exact method based on the Wiener-Hopf method [9, 10] showed an excellent agreement along the whole front arc, not only at high frequencies but also at low frequencies. The accuracy of the directivity starts to decrease above an angle of 100^o with respect to the cylinder axis. In and beyond this zone, the pressure levels range between 10 dB and 50 dB below the sound pressure levels originating from the other part of the engine, which means that the inaccuracy of the approximation in this region is irrelevant to the total sound pressure field.

2 Theoretical developments

2.1 Geometry and notations

Let us consider an infinite domain where the reference coordinates defined as cartesian (O, x, y, z), cylindrical (O, r, θ, z) or spherical $(0, r, \theta, \varphi)$. This domain contains a fluid defined by its sound speed c_e and its density ρ_e. This fluid has a uniform motion at a speed of $U_e < c_e$ (with Mach number $M_e = U_e/c_e < 1$) parallel to the z-axis. This domain contains at the origin two rigid cylindrical pipes of finite length with different diameters: R_1 in the case of the upstream pipe (at the intake end of the engine) and R_2 in that of the downstream pipe (at the exhaust end of the engine). With the model developed here, the length of these pipes has no importance. This picture does not include the interference introduced by the acoustic fields, but this seems to be of little practical importance because it is impossible to fix the relative phases corresponding to the various acoustic sound pressure fields *a priori* . The downstream pipe is extended by an infinite cylindrical fluid with radius R_2 containing a fluid with sound speed c_i and density ρ_i with a uniform speed U_i parallel to the z-axis (Mach number $M_i = U_i/c_i < 1$). S_e is the section of the waveguide and S is the external part of the cylinder (see figure 1).

Here we examine the acoustic sound pressure $p(Q, t)$ at an observation point Q located outside the engine, and moving with the flow at Mach number M_e. The fixed engine/moving observer system is equivalent to a system consisting of an engine moving at Mach M_e and a fixed observer in a still space (for example standing on the ground). Point Q is described by its spherical coordinates R_e, θ, φ_e downstream and R_a, θ, φ_a upstream. These two systems of coordinates are only introduced

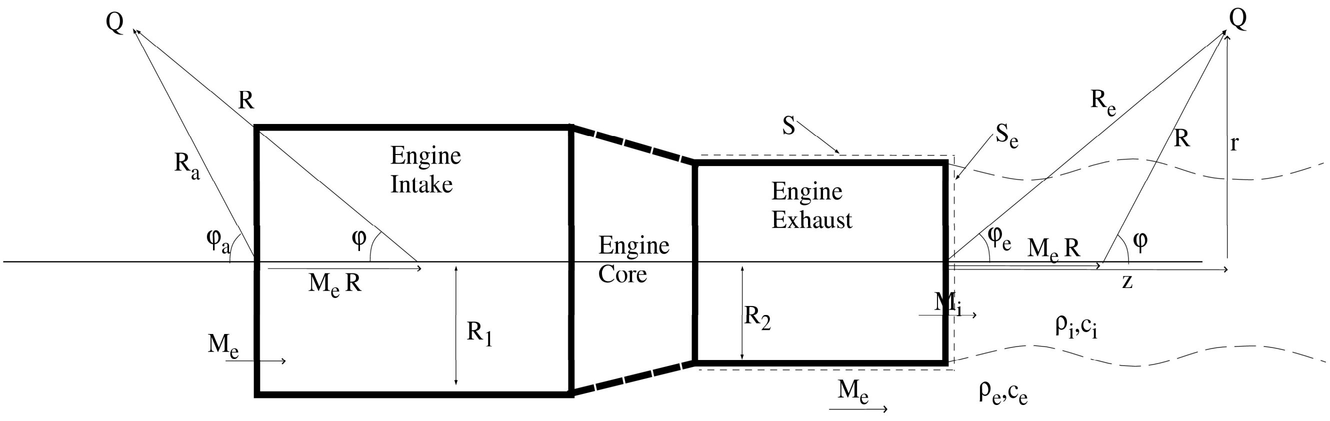

Figure 1: Geometry

to facilitate the subsequent calculations. To simplify the calculations as well as to the results easier to interpret, it is convenient to introduce a coordinate system based on the reception time [6]. In the observer's time, the coordinates of Q are R, θ, φ. One has:

$$
\begin{aligned}
R_{a,e} &= \sqrt{R^2 \sin^2\varphi + R^2(\pm M_e + \cos^2\varphi)^2} \\
&= R\sqrt{1 + M_e^2 \pm 2M_e \cos^2\varphi}, \begin{cases} + \text{ for } R_a \\ - \text{ for } R_e \end{cases} \\
\sin\varphi_{a,e} &= \frac{R\sin\varphi}{R_{a,e}} \\
&= \frac{\sin\varphi}{\sqrt{1 + M_e^2 \pm 2M_e \cos^2\varphi}}
\end{aligned}
$$

2.2 Equations expressing the problem

2.2.1 Equation of wave propagation outside a moving surface

In this part, we recall Cargill's theory [3].

The acoustic sound pressure in the case of a fluid moving at uniform speed U parallel to the z axis, is the solution of the convected wave equation

$$\left(\Delta - \frac{1}{c^2}\left(\frac{\partial}{\partial t} + U\frac{\partial}{\partial z}\right)^2\right) p(M,t) = 0 \tag{1}$$

Let us take $\frac{D}{Dt} = \frac{\partial}{\partial t} + U\frac{\partial}{\partial z}$ to denote the particular derivative. To obtain the acoustic pressure field outside a mobile surface (the engine) defined by $f = 0$ with $f > 0$ outside the surface and $f < 0$ inside the surface, we multiply equation (1) by $H(f)$ where $H(x)$ is the Heaviside step function. This gives

$$H(f)\left(\Delta p(M,t) - \frac{1}{c^2}\frac{Dp(M,t)}{Dt}\right) = 0$$

but

$$\begin{aligned} H\Delta p &= \Delta(pH) - \operatorname{div}(p\overline{\nabla}H) - \overline{\nabla}p\cdot\overline{\nabla}H \\ H\frac{D^2p}{Dt^2} &= \frac{D^2pH}{Dt^2} - \frac{D}{Dt}\left(p\frac{DH}{Dt}\right) + \frac{DH}{Dt}\frac{Dp}{Dt} \end{aligned}$$

Then

$$\begin{aligned} \left(\Delta - \frac{1}{c^2}\frac{D}{Dt}\right)(p(M,t)H(f)) &= \operatorname{div}(p(M,t)\overline{\nabla}H(f)) + \overline{\nabla}p(M,t)\cdot\overline{\nabla}H(f) \\ &\quad -\frac{1}{c^2}\left(\frac{D}{Dt}\left(p(M,t)\frac{DH(f)}{Dt}\right) + \frac{DH(f)}{Dt}\frac{Dp(M,t)}{Dt}\right) \\ &= f^s \end{aligned} \tag{2}$$

Equation (2) is used to calculate the acoustic sound pressure field radiated by each portion of the engine in term of the Kirchhoff approximation. For example, at the exhaust, the moving surface can be assumed to constist of the pipe S and its exit section S_e. By definition, the normal derivative of the pressure is zero on S. In the Kirchhoff approximation, the pressure is also taken to be zero at the surface of the pipe. The only acoustic source is therefore that formed by the exit section of the pipe S_e, the pressure and normal derivative of which are those of the incident field inside the pipe.

Let us take the Green's function $G(M,t;M_0,t_0)$, where the particle displacement and acoustic pressure are continuous across the jet, which satisfies

$$\begin{aligned} \left(\Delta_M - \frac{1}{c_i^2}\frac{D_i}{Dt}\right)G(M,t;M_0,t_0) &= \delta_{M_0}(M)\delta_{t_0}(t), \text{ inside the jet} \\ \left(\Delta_M - \frac{1}{c_e^2}\frac{D_e}{Dt}\right)G(M,t;M_0,t_0) &= 0, \text{ outside the jet} \end{aligned}$$

with $\frac{D_{e,i}}{Dt} = \frac{\partial}{\partial t} + U_{e,i}\frac{\partial}{\partial z}$.

To establish the Green's representation for the pressure, we start with equation (2 written as follows: $\left(\Delta - \frac{1}{c^2}\frac{D}{Dt}\right)\delta \star (pH) = f^s$, where $\star$ is the convolution product in time and space extended to the whole volume V of the jet. This gives $G \star \left(\Delta - \frac{1}{c^2}\frac{D}{Dt}\right)\delta \star (pH) = G \star f^s = p$. By expanding the convolution product, one obtains:

$$\begin{aligned} p(M,t) &= \int_{V,t} G(M,t;M',t')(\mathrm{div}(p(M',t')\overline{\nabla}H(f)) + \overline{\nabla}p(M',t')\overline{\nabla}H(f))\mathrm{d}M'\mathrm{d}t' \\ &\quad -\frac{1}{c^2}\int_{V,t} G(M,t;M',t')\left(\frac{D}{Dt'}\left(p(M',t')\frac{DH(f)}{Dt'}\right) + \frac{DH(f)}{Dt'}\frac{Dp(M',t')}{Dt'}\right)\mathrm{d}M'\mathrm{d}t' \end{aligned}$$

while integrating by parts, we obtain:

$$\begin{aligned} \int_{V,t} G(M,t;M',t')\mathrm{div}(p(M',t')\overline{\nabla}H(f))\mathrm{d}M'\mathrm{d}t' &= \int_{V,t} \mathrm{div}(G(M;t,M',t')p(M',t')\overline{\nabla}H(f)\mathrm{d}M'\mathrm{d}t' \\ &\quad -\int_{V,t} p(M',t')\overline{\nabla}_{M'}G(M,t;M',t')\cdot\overline{\nabla}H(f)\mathrm{d}M'\mathrm{d}t' \\ &= -\int_{V,t} p(M',t')\overline{\nabla}_{M'}G(M,t;M',t')\cdot\overline{\nabla}H(f)\mathrm{d}M'\mathrm{d}t' \end{aligned}$$

Likewise, we have:

$$\begin{aligned} \int_{V,t} G(M,t;M',t')\frac{D\left(p(M',t')\frac{DH(f)}{Dt'}\right)}{Dt'}\mathrm{d}M'\mathrm{d}t' &= \int_{V,t}\frac{D}{Dt'}\left(G(M,t;M',t')p(M',t')\frac{DH(f)}{Dt'}\right)\mathrm{d}M'\mathrm{d}t' \\ &\quad -\int_{V,t}\frac{DG(M,t;M',t')}{Dt'}p(M',t')\frac{DH(f)}{Dt'}\mathrm{d}M'\mathrm{d}t' \\ &= -\int_{V,t}\frac{DG(M,t;M',t')}{Dt'}p(M',t')\frac{DH(f)}{Dt'}\mathrm{d}M'\mathrm{d}t' \end{aligned}$$

Finally:

$$\begin{aligned} p(M,t) &= \int_{V,t}(G(M,t;M',t')\overline{\nabla}p(M',t') - p(M',t')\overline{\nabla}_{M'}G(M,t;M',t'))\cdot\overline{\nabla}H(f))\mathrm{d}M'\mathrm{d}t' \\ &\quad -\frac{1}{c^2}\int_{V,t}\left(G(M,t;M',t')\frac{Dp(M',t')}{Dt'} - p(M',t')\frac{DG(M,t;M',t')}{Dt'}\right)\frac{DH(f)}{Dt'}\mathrm{d}M'\mathrm{d}t'. \end{aligned}$$

2.3 Sound pressure radiated by the engine

As an example, let us consider the downstream part of the engine. In this case, one can set the position of S_e at $z = 0$. One has $\overline{\nabla}H(f)) = \overline{n}\delta(z)$ and $\frac{DH(f)}{Dt} = U_i\delta(z)$, where $\overline{n}$ is the normal to

S_e and $\delta(z)$ is the Dirac delta distribution at $z=0$. Taking into account the Neumann condition and the zero pressure condition on the external surface S, one obtains the Kirchhoff formula for a moving surface [7] :

$$\begin{aligned} p_e(M,t) &= \int_{S_e,t} (G(M,t;M',t')\partial_{\overline{n}} p_e(M',t') - p_e(M',t')\partial_{\overline{n}(M')} G(M,t;M',t'))\ \mathrm{d}M'\mathrm{d}t' \\ &- \frac{1}{c_i^2}\int_{S_e,t}\left(G(M,t;M',t')\frac{D_i p_e(M',t')}{Dt'} - p_e(M',t')\frac{D_i G(M,t;M',t')}{Dt'}\right) U_i \mathrm{d}M'\mathrm{d}t'. \end{aligned}$$

Thanks to the 2π-periodicity in θ of the geometry, all the quantities involved in the problem can be expanded into angular Fourier series:

$$f(r,\theta,z/\varphi) = \sum_{m=-\infty}^{m=+\infty} f_m(r,z/\varphi)\mathrm{e}^{\imath m\theta}$$

Let us now assume that the time dependency is harmonic: $\mathrm{e}^{-\imath\omega t}$. The acoustic pressure outside the pipe is then given by:

$$\begin{aligned} p_{me}(r,z) &= \int_0^{R_2}\left(G_m(r,z;r_0,z_0)\frac{\partial}{\partial z_0}p_{me}(r_0,z_0) - p_{me}(r_0,z_0)\frac{\partial}{\partial z_0}G_m(r,z;r_0,z_0)\right)_{z_0=0} r_0\mathrm{d}r_0 \\ &- \frac{U_i}{c_i^2}\int_0^{R_2}\left(G_m(r,z;r_0,z_0)\frac{D_i p_{me}(r_0,z_0)}{Dt_0} - p_{me}(r_0,z_0)\frac{D_i G_m(r,z;r_0,z_0)}{Dt_0}\right)_{z_0=0} r_0\mathrm{d}r_0 \quad (3) \end{aligned}$$

where $\frac{D_i}{Dt_0} = -\imath\omega + U_i\frac{\partial}{\partial z_0}$.

By continuity, if no reflection of the incident pressure occurs at the exit plane (this is valid only when the operating frequency is much higher than the cut-off frequency of the mode considered), one has on the exit plane of the pipe

$$\begin{aligned} p_{me}(r_0,z_0) &= p_{mi}(r_0,z_0) \text{ at } z_0=0 \\ \partial_{z_0}p_{me}(r_0,z_0) &= \partial_{z_0}p_{mi}(r_0,z_0) \text{ at } z_0=0 \end{aligned}$$

where $p_{mi}(r,z)$ is the incident pressure inside the pipe. Obviously, near the cut-off, a significant reflection occurs and these results are therefore not valid. Let us now assume that the incident pressure field is given by a propagating mode with index (m,n) and wavenumber k^e_{mn} [7, 8]:

$$p_{mi}(r,z) = \mathrm{J}_m(j'_{mn}\frac{r}{R_2})\mathrm{e}^{\imath k^e_{mn}z}, \text{ where } k^e_{mn} = \frac{k^i_0}{\beta_i^2}\left(-M_i + \sqrt{1-\left(\beta_i\frac{\kappa^i_{mn}}{k^i_0}\right)^2}\right)$$

where $k_0^i = \omega/c_i$, $\beta_i = \sqrt{1-M_i^2}$ and $\kappa^i_{mn} = j^{'}_{mn}/R_2$. $\mathrm{J}_m(z)$ is the Bessel function.

One has (see Appendix) :

$$G_m(r,z;r_0,z_0) = -\frac{\imath}{4}\int_{-\infty}^{\infty} \mathrm{H}_m(\kappa_e r)T_m(k_z)\mathrm{J}_m(\kappa_i r_0)\mathrm{e}^{\imath k_z(z-z_0)}\mathrm{d}k_z \tag{4}$$

where $\mathrm{H}_m(z)$ is the Hankel function of the first kind and $T_m(k_z)$ is the transmission coefficient of the jet. Using the continuity relations and the expressions for the incident pressure fields and Green's function, one obtains the pressure outside the downstream pipe:

$$\begin{aligned}
p_{me}(r,z) \;=\; & -\frac{\imath}{4}\int_0^{R_2}\Big\{\int_{-\infty}^{\infty}\mathrm{H}_m(\kappa_e r)T_m(k_z)\mathrm{J}_m(\kappa_i r_0)\mathrm{e}^{\imath k_z z}\mathrm{d}k_z(\imath k^e_{mn})\mathrm{J}_m(j^{'}_{mn}\frac{r_0}{R_2}) \\
& \qquad - (-\imath k_z)\mathrm{J}_m(j^{'}_{mn}\frac{r_0}{R_2})\int_{-\infty}^{\infty}\mathrm{H}_m(\kappa_e r)T_m(k_z)\mathrm{J}_m(\kappa_i r_0)\mathrm{e}^{\imath k_z z}\mathrm{d}k_z\Big\}\,r_0\mathrm{d}r_0 \\
& +\frac{\imath}{4}\frac{U_i}{c_i^2}\int_0^{R_2}\Big\{\int_{-\infty}^{\infty}\mathrm{H}_m(\kappa_e r)T_m(k_z)\mathrm{J}_m(\kappa_i r_0)\mathrm{e}^{\imath k_z z}\mathrm{d}k_z(-\imath\omega+\imath U_i k^e_{mn})\mathrm{J}_m(j^{'}_{mn}\frac{r_0}{R_2}) \\
& \qquad - \mathrm{J}_m(j^{'}_{mn}\frac{r_0}{R_2})(-\imath\omega-\imath U_i k_z)\int_{-\infty}^{\infty}\mathrm{H}_m(\kappa_e r)T_m(k_z)\mathrm{J}_m(\kappa_i r_0)\mathrm{e}^{\imath k_z z}\mathrm{d}k_z\Big\}\,r_0\mathrm{d}r_0
\end{aligned}$$

And by rearranging the terms :

$$\begin{aligned}
p_{me}(r,z) \;=\; & -\frac{\imath}{4}\int_{-\infty}^{\infty}\Bigg[T_m(k_z)\left\{-\imath(-k_z-k^e_{mn})+\imath\frac{U_i}{c_i^2}\left[(\omega-U_ik^e_{mn})-(\omega+U_ik_z)\right]\right\} \\
& \qquad \int_0^{R_2}\mathrm{J}_m(\kappa_i r_0)\mathrm{J}_m(j^{'}_{mn}\frac{r_0}{R_2})r_0\mathrm{d}r_0\ \mathrm{H}_m(\kappa_e r)\mathrm{e}^{\imath k_z z}\Bigg]\,\mathrm{d}k_z.
\end{aligned}$$

But since we know [1] that $\int(\beta^2-\alpha^2)z\mathrm{J}_m(z\alpha)\mathrm{J}_m(\beta z)\mathrm{d}z = z\left(\alpha\mathrm{J}'_m(\alpha z)\mathrm{J}_m(\beta z)-\beta\mathrm{J}_m(\beta z)\mathrm{J}'_m(\alpha z)\right)$ then

$$\int_0^{R_2}\mathrm{J}_m(\kappa_i r_0)\mathrm{J}_m(j^{'}_{mn}\frac{r_0}{R_2})r_0\mathrm{d}r_0 = -\frac{R_2\kappa_i}{\kappa_i^2-\left(\frac{j^{'}_{mn}}{R_2}\right)^2}\mathrm{J}_m(\kappa_i R_2)\mathrm{J}_m(j^{'}_{mn})$$

Finally, the acoustic pressure outside the jet is given by:

$$\begin{aligned}
p_{me}(r,z) \;=\; & -\frac{\imath}{4}\int_{-\infty}^{\infty}\Bigg[T_m(k_z)\left\{-\imath(-k_z-k^e_{mn})+\imath\frac{U_i}{c_i^2}\left[(\omega-U_ik^e_{mn})-(\omega+U_ik_z)\right]\right\} \\
& \qquad \frac{-R_2\kappa_i}{\kappa_i^2-\left(\frac{j^{'}_{mn}}{R_2}\right)^2}\mathrm{J}_m(\kappa_i R_2)\mathrm{J}_m(j^{'}_{mn})\ \mathrm{H}_m(\kappa_e r)\mathrm{e}^{\imath k_z z}\Bigg]\,\mathrm{d}k_z,
\end{aligned} \tag{5}$$

with $\kappa_{i,e} = \kappa_{i,e}(k_z)$. This result is valid only for subsonic flows but it is valid for identical Mach numbers (where the transmission coefficient $T_m(k_z) = 1$) and even for zero Mach numbers.

Now to compute the acoustic pressure radiated by the upstream part of the engine, one can either use this result directly (by imposing $M_i = M_e$) or use the Prandtl-Glauert's transformation which consists in calculating the sound pressure field in the moving reference frame, taking $M_i = M_e = 0$ in equation (5). Because of its simplicity, this latter method is used.

2.4 Directivity of the aeroengine

2.4.1 Exhaust of the engine

Let us now consider the far field $R/R_{1,2} \gg 1$ and $kR \gg 1$. In the reception coordinate system (cf. figure 1), the cylindrical coordinates of the point Q are given by $(r, \theta, z) = (R\sin\varphi, \theta, R(M_e + \cos\varphi))$. Sufficiently far from the jet axis, one has $r = R\sin\varphi \gg 1$. By performing asymptotic expansion, we obtain$\mathrm{H}_m(\kappa_e r) \approx \sqrt{2/(\pi\kappa_e r)}\exp\imath(\kappa_e r - m\pi/2 - \pi/4)$. Equation (5) is then written

$$p_{me}(r,z) = \int_{-\infty}^{\infty} f_m(k_z)\mathrm{e}^{\imath(\kappa_e r - k_z z)}\mathrm{d}k_z. \tag{6}$$

with

$$\begin{aligned} f_m(k_z) \quad = \quad & -\frac{\imath}{4}T_m(k_z)\left\{-\imath(-k_z - k^e_{mn}) + \imath\frac{U_i}{c_i^2}\left[(\omega - U_i k^e_{mn}) - (\omega + U_i k_z)\right]\right\} \\ & \frac{-R_2\kappa_i}{\kappa_i^2 - \left(\frac{j'_{mn}}{R_2}\right)^2}\mathrm{J}_m(\kappa_i R_2)\mathrm{J}_m(j'_{mn})\sqrt{\frac{2}{\pi\kappa_e r}}\mathrm{e}^{-\imath(m\frac{\pi}{2}+\frac{\pi}{4})}. \end{aligned}$$

The exponential term can be written:

$$\mathrm{e}^{\imath(\kappa_e r - k_z z)} = \mathrm{e}^{\imath R(\kappa_e(k_z)\sin\varphi - k_z(M_e + \cos\varphi))} = \mathrm{e}^{\imath R h(k_z)},$$

this gives:

$$p_{me}(r,z) = p_{me}(R,\varphi) = \int_{-\infty}^{\infty} f_m(k_z)\mathrm{e}^{\imath R h(k_z)}\mathrm{d}k_z.$$

By applying the stationary phase method [6], we obtain:

$$p_{me}(R,\varphi) \approx f_m(k_z^0)\sqrt{\frac{2\pi}{R\,|h''(k_z^0)|}}\mathrm{e}^{\imath R h(k_z^0) + \imath\,\mathrm{sgn}(h''(k_z^0))\frac{\pi}{4}}$$

if $h'(k_z^0) = 0$ and $h''(k_z^0) \neq 0$.

It can easily be established that

$$k_z^0 = -k_0^e \frac{\cos\varphi}{(1 + M_e \cos\varphi)}$$

where $k_0^e = \omega / c_e$. $h(k_z^0) = k_0^e$ and $h''(k_z^0) = -(1 + M_e \cos\varphi)^3 / (k_0^e \sin\varphi)^2 < 0$. Then finally:

$$p_{me}(R, \varphi) \approx f_m(k_z^0) \sqrt{\frac{2\pi (k_0^e \sin\varphi)^2}{R (1 + M_e \cos\varphi)^3}} \mathrm{e}^{\imath R k_0^e} \mathrm{e}^{-\imath \frac{\pi}{4}}.$$

Now, still in line with Cargill's method, let us denote

$$\begin{aligned} \chi_0(k_z^0) &= -k_z^0 + M_i (k_0^i + M_i k_z^0), \\ \chi_{mn}(k_z^0) &= -k_{mn}^e - M_i (k_0^i - M_i k_{mn}^e), \end{aligned}$$

and

$$\begin{aligned} D_m(k_z^0) &= -\imath R_2 (\chi_0(k_z^0) + \chi_{mn}(k_z^0)), \\ I_m(k_z^0) &= \frac{-2 R_2 \kappa_i(k_z^0)}{\kappa_i^2(k_z^0) R_2^2 - j_{mn}'^2} \mathrm{J}_m(\kappa_i(k_z^0) R_2) \mathrm{J}_m(j_{mn}'). \end{aligned}$$

Then finally

$$\begin{aligned} p_{me}(R, \varphi) &\approx -\frac{\mathrm{e}^{\imath R k_0^e}}{4\pi R} T_m(k_z^0) D_m(k_z^0) I_m(k_z^0) \frac{\pi R_2}{1 + M_e \cos\varphi} \mathrm{e}^{-\imath m \frac{\pi}{2}} \\ &= -\frac{\mathrm{e}^{\imath R k_0^e}}{4\pi R} \Xi_{mn}^e(k_0^e, \varphi). \end{aligned} \tag{7}$$

$\Xi_{mn}^e(k_0^e, \varphi)$ is the directivity diagram of the engine exhaust.

2.4.2 Intake of the engine

To calculate the sound pressure emitted at engine intake end, we apply the theory of Candel [2] or Homicz and Lordi [11] which consists in solving the problem for a medium at rest with the following variables:

$$\cos\varphi_{1a} = \frac{\cos\varphi_a}{\sqrt{1 - M_e^2 \sin^2\varphi_a}}, \sin\varphi_{1a} = \frac{\beta_e \sin\varphi_a}{\sqrt{1 - M_e^2 \sin^2\varphi_a}}$$

$$\begin{aligned} k_1^e &= \frac{k_0^e}{\beta_e}, \beta_e = \sqrt{1-M_e^2} \\ R_{1a} &= \frac{R_a}{\beta_e}\sqrt{1-M_e^2\sin^2\varphi_a} = \frac{R}{\beta_e}\sqrt{1+M_e^2-2M_e\cos\varphi}\sqrt{1-M_e^2\sin^2\varphi_a} \end{aligned}$$

with (see figure 1) $\sin\varphi_a = \sin\varphi/\sqrt{1+M_e^2 \pm 2M_e\cos^2\varphi}$.

This gives:

$$p_{ma}(R,\varphi) \approx -\frac{\mathrm{e}^{\imath R_{1a}k_1^e}}{4\pi R_{1a}}\Xi^0_{mn}(k_1^e,\varphi_{1a})\frac{1-M_e\cos\varphi_a}{1-M_e\sqrt{1-\left(\frac{j'_{mn}}{k_1^e R_1}\right)^2}} \tag{8}$$

where $\Xi^0_{mn}(k,\varphi)$ is the directivity diagram of the upstream pipe calculated without any flow, which is obtained simply by taking the Mach numbers M_i and M_e to be equal to zero in $\Xi^e_{mn}(k_0^e,\varphi)$. It is worth noting that in this case, the incident pressure wave is given by the propagating mode (m,n) with wavenumber k^a_{mn}

$$p_{mi}(r,z) = \mathrm{J}_m(j'_{mn}\frac{r}{R_1})\mathrm{e}^{-\imath k^a_{mn}z}, \text{ where } k^a_{mn} = k_0^e\left(\sqrt{1-\left(\frac{\kappa^i_{mn}}{k^i_0}\right)^2}\right)$$

where $k_0^i = \omega/c_i$ and $\kappa^i_{mn} = j'_{mn}/R_1$.

Upon carrying into equation (8) the various expressions for the transformed variables, the exponential term becomes:

$$-\frac{\mathrm{e}^{\imath R_{1a}k_1^e}}{4\pi R_{1a}} = -\frac{\mathrm{e}^{\imath\frac{R}{\beta_e}k_0^e\sqrt{1-M_e^2\sin^2\varphi_a}\sqrt{1+M_e^2-2M_e\cos\varphi}}}{4\pi\frac{R}{\beta_e}\sqrt{1-M_e^2\sin^2\varphi_a}\sqrt{1+M_e^2-2M_e\cos\varphi}}$$

Since only the amplitude is significant in the calculation of the directivity one can neglect the phase term in the previous relation (this approximation becomes exact when the Mach number is zero). One then obtains:

$$-\frac{\mathrm{e}^{\imath R_{1a}k_1^e}}{4\pi R_{1a}} \approx -\frac{\mathrm{e}^{\imath k_0^e R}}{4\pi R}\frac{\sqrt{1-M_e^2}}{\sqrt{1-M_e^2\sin^2\varphi_a}\sqrt{1+M_e^2-2M_e\cos\varphi}}$$

Finally, by reporting this result into equation (8) :

$$\begin{aligned} p_{ma}(R,\varphi) &\approx -\frac{\mathrm{e}^{\imath k_0^e R}}{4\pi R}\Xi^0_{mn}(k_1^e,\varphi_{1a})\frac{1-M_e\cos\varphi_a}{1-M_e\sqrt{1-\left(\frac{j'_{mn}}{k_1^e R_1}\right)^2}}\frac{\sqrt{1-M_e^2}}{\sqrt{1-M_e^2\sin^2\varphi_a}\sqrt{1+M_e^2-2M_e\cos\varphi}} \\ &\approx -\frac{\mathrm{e}^{\imath k_0^e R}}{4\pi R}\Xi^a_{mn}(k_0^e,\varphi) \end{aligned} \tag{9}$$

$\Xi^a_{mn}(k_0^e,\varphi)$ is the directivity function of the upstream part of the engine in a uniform flow.

2.4.3 The complete directivity

To obtain the directivity of the complete engine, the two partial directivities are simply added, taking the upstream change of variable into account. If the origin of the angular variable φ is fixed downstream, one has:

$$p_{ma}(R,\varphi) \approx -\frac{\mathrm{e}^{\imath k_0^e R}}{4\pi R}\left(\Xi_{mn}^a(k_0^e,\pi-\varphi)+\Xi_{mn}^e(k_0^e,\varphi)\right) \tag{10}$$

2.4.4 Maximum directivity of the engine

It can easily be seen that the engine has two directivity maxima, one at each of its ends. Let us take φ_{mn}^{pa} to denote the maximum at the intake end, as previously proposed by Candel [2] and Homicz and Lordi [11], and φ_{mn}^{pe} to denote the maximum at the exhaust end.

To calculate φ_{mn}^{pa}, let us start by looking for the angle of the maximum directivity without flow, denoted φ_{mn}^{p}. It can be easily seen that $kR_1\sin\varphi_{mn}^{p} = j_{mn}^{'}$. With flow, in line with Candel, one has $k_1^e R_1 \sin\varphi_{mn1a}^{pa} = j_{mn}^{'}$. From $\sin\varphi_{mn1a}^{pa} = \beta_e \sin\varphi_{mna}^{pa}/\sqrt{1-M_e^2\sin^2\varphi_{mna}^{pa}}$, one obtains $\sin\varphi_{mna}^{pa} = (j_{mn}^{'}/(kR_1))^2/\sqrt{1+M_e^2(j_{mn}^{'}/(kR_1))^2}$. From $\sin\varphi_{mna}^{pa} = \sin\varphi_{mn}^{pa}/\sqrt{1+M_e^2\pm 2M_e\cos^2\varphi_{mn}^{pa}}$, one obtains a quadratic equation in term of $\cos\varphi_{mn}^{pa}$:

$$\cos^2\varphi_{mn}^{pa} - 2M_e\gamma\cos\varphi_{mn}^{pa} + \gamma(1+M_e^2) - 1 = 0,$$

with $\gamma = (j_{mn}^{'}/(kR_1))^2/(1+M_e^2(j_{mn}^{'}/(kR_1))^2)$. then :

$$\varphi_{mn}^{pa} = \arccos\left(M_e\gamma + \sqrt{(1-M_e^2\gamma)(1-\gamma)}\right) \tag{11}$$

By a similar way, it can be easily established that φ_{mn}^{pe} corresponds to the maximum of $I_m(k_z^0)$. This occurs when $\kappa_i^2(k_z^{0pe})R_2^2 = j_{mn}^{'2}$ with $k_z^{0pe} = -k_0^e\frac{\cos\varphi_{mn}^{pe}}{(1+M_e\cos\varphi_{mn}^{pe})}$. From $\kappa_i^2(k_z) = (k_0^i + M_i k_z)^2 - k_z^2$, one again obtains a quadratic equation in term of $\cos\varphi_{mn}^{pe}$:

$$(M_\alpha^2 - \alpha_c^2 - \alpha_{mn}^2 M_e^2)\cos^2\varphi_{mn}^{pe} + 2(M_\alpha - \alpha_{mn}^2 M_e)\cos\varphi_{mn}^{pe} + 1 - \alpha_{mn}^2 = 0,$$

with $\alpha_c = c_i/c_e$, $M_\alpha = M_e - \alpha_c M_i$ and $\alpha_{mn} = j'_{mn}/(k_0^i R_2)$. Then, one obtains

$$\varphi_{mn}^{pe} = \arccos\left(\frac{\alpha_{mn}^2 M_e - M_\alpha + \sqrt{(M_\alpha - \alpha_{mn}^2 M_e)^2 - (1-\alpha_{mn}^2)(M_\alpha^2 - \alpha_c^2 - \alpha_{mn}^2 M_e^2)}}{M_\alpha^2 - \alpha_c^2 - \alpha_{mn}^2 M_e^2}\right) \tag{12}$$

3 Results and comments

Here we present some examples in the case of an engine where the intake radius is set at a value of $R_1 = 0,086$. The exhaust radius R_2 has fixed values of R_1 in all the figures except for figures 11 and 12, where it has the following values $R_2 = R_1$, $R_2 = R_1 \times 0.9$, $R_2 = R_1 \times 0.75$ and $R_2 = R_1 \times 0.5$. The internal and external fluids are both air ($\rho_{i,e} = 1,3$, $c_{i,e} = 330m/s$). In the various examples, we consider two modes: the mode $(3,2)$ the cut-off frequency of which is given by $\kappa_{32}^i R = j'_{32} = 8.015$ and the $(4,1)$ mode the cut-off frequency of which is given by $\kappa_{41}^i R = j'_{41} = 5.318$. The computations were carried out using the Mathematica software program on a personal computer; each run, consisting of about twenty lines, takes a few seconds. Two kinds of results are presented. The first set (figures 3, 4, 5, 6 and 7) shows the evolution of the maximum directivity upstream and downstream with respect to the Mach numbers and frequency. The second set of results (figures 8 to 16) give the evolution of the directivity of the aeroengine at various Mach numbers and intake and exhaust radii; this is done with three frequencies $kR_1 = 11.7$ in figures 8 to 12, $kR_1 = 12.47$ in figures 13 and 14 and $kR_1 = 23.43$ in figures 15 and 16.

In the figures giving the second set of results, except for figure 16 for the highest external Mach number (see next paragraph), one can see the two directivity maxima, corresponding to the two ends of the engine. As shown by the equations, the maximum at the exhaust end ($\varphi^{pe} \approx 30^o$) depends on the difference between the jet's internal and external Mach numbers.

One interesting aspect of the problem is illustrated in equation (12). Since the argument of the inverse cosine function could be larger than unity, the maximum φ_{mn}^{pe} could not exist. This can be seen in figures 6, 10 and 16 at the highest external Mach number, where there is an external Mach number above which the maximum directivity of the exhaust merges with the axis of the jet. At a ratio of wave speeds α_c close to one, there always exists a combination of parameters α_{mn}, M_e and M_i at which φ_{mn}^{pe} tends to zero. The three possibilities are given below:

$$\begin{aligned} M_e &> \frac{1 - M_i\alpha_c - \alpha_{mn}^2 - \alpha_c\sqrt{1 + (M_i^2 - 1)\alpha_{mn}^2}}{\alpha_{mn}^2 - 1}, \text{ for } \alpha_c \text{ and } M_i \text{ fixed} \\ M_i &> \frac{1 + M_e - \sqrt{\alpha_c^2 + (1 + M_e^2)\alpha_{mn}^2}}{\alpha_c}, \text{ for } \alpha_c \text{ and } M_e \text{ fixed} \\ \alpha_{mn} &< \frac{\sqrt{1 + M_e^2 - 2M_i\alpha_c - \alpha_c^2 + M_i^2\alpha_c^2 + 2M_e(1 - M_i\alpha_c)}}{1 + M_e}, \text{ for } M_i \text{ and } M_e \ (M_i < M_e) \text{ are fixed.} \end{aligned}$$

The latter result means that when α_c is close to one and $M_i < M_e$ at high frequencies the mode does not radiate far into the external fluid and the jet serves as a waveguide. This can be seen from figure 6, where one can see that when a sufficiently large difference exists between the two Mach numbers at high frequencis, the sound radiated by the exhaust part of the engine is well below that occuring at the intake end.

Figure 8 is presented the sake of comparison, based on the same parameters as those used by Cargill [3] in his figure 2. As noted by Cargill upon comparing his results with the exact ones obtained using a Wiener-Hopf solution, “the agreement is exceptionally good until an angle of 100^o is reached”. And it is clear from figure 8 that even at an angle of 90^o to the jet axis, the radiation from the exhaust is completely swamped by the the radiation from the intake. Figure 9 shows the influence of the exhaust jet in the engine at rest. Except in the cone of silence (corresponding to $\kappa_i^2(k_z^0)$), which widens with the internal Mach number, the maximum level remains practically constant and is shifted to the side. Figures 10, 13 and 14 show the effects of the external Mach number. Here one can see the classical (see for example chapter 14 in [6]) change in the pressure level resulting from the subsonic movement of the engine which increases the sound pressure level radiated by the intake engine and decreases the sound radiated by the exhaust. In addition to these effects, the shift toward the axis of the engine of the maximum radiation of the intake predicted by equation (11) can be clearly observed.

Figures 11 and 12 show the influence of the change of exhaust radius size on the directivity of the engine at rest (figure 11) and moving (figure 11). In all the cases studied, the smaller the exhaust radius was, the quieter the engine became. The change in the shape of the directivity was particularly interresting. As long as the radius of the exhaust is similar to that of the intake, the sound level decreases possibly due to a spreading of energy. But when the exhaust radius becomes twice as small as the intake radius, a dramatic change occurs, the sound pressure radiated by the exhaust becomes very small, and the sound radiated by the engine at the exhaust end practically equal to the intake level. This can be seen from the two figures in which the directivity of the intake has been plotted, at small exhaust radius, the directivity of the engine can be seen to be practically equals to the intake level ones.

Figures 15 and 16 differ only in the internal Mach number which is smaller in figure 16, where the maximum directivity disappears.

4 Conclusion

There we propose an expression for the far field acoustic sound pressure radiated at high frequency by an aeroengine under flight conditions. This expression takes into account some of the main features of a true engine: the intake and exhaust diameter differ and an exhaust jet is present. Studies can easily be conducted on many parameters not mentioned here such as the influence of the diameter of each part of the engine, the influence of the relative Mach numbers, and the change in the properties of the fluid inside the jet, or a multi modal analysis could be carried out. Some other important features have not yet been taken into account, such as the presence of a secondary annular exhaust jet, the influence of the length of the engine, the presence of the wing or the axial and radial change in the velocity profile inside the pipe (see for example [24]). But since they are so difficult to approach, these aspects can probably only be handled by developing complex programs involving finite or boundary elements which would make the numerical computational cost of these studies prohibive.

5 Acknowledgment

The author would like to thank the French *Ministère de la Recherche* for funding part of this research project via the *Réseau de recherche sur l'avion supersonique.*

References

[1] M. Abramowitz and I. A. Stegun 1965. *Handbook of Mathematical Functions.* New-York : Dover.

[2] S. M. Candel. Acoustic Radiation from the end of a two-dimensional duct, effects of uniform flow and duct lining. *Journal of Sound and Vibration* 28(1) (1973) 1-13.

[3] A. M. Cargill. The radiation of high frequency sound out of jet pipe. *Journal of Sound and Vibration* 83(3) (1982) 313-337.

[4] A. M. Cargill. Low frequency acoustic radiation from a jet pipe - A second order theory. *Journal of Sound and Vibration* 83(3) (1982) 339-354.

[5] G. F. Carrier. Sound transmission from a tube with flow. *Quarterly of Applied Mathematics* 13 (1956) 457-461.

[6] D.G. Crighton, A.P. Dowling, J.E. Ffowcs Williams, M. Heckl and F.G. Leppigton. Chapter 14 : Effect of motion on acoustics sources. *Modern Method in Analytical Acoustics.* Springer-Verlag. (1992).

[7] F. Farassat. The Kirchhoff formulas for moving surface in aeroacoustic - the subsonic and supersonic cases. *NASA technical memorandum 110285* (1996).

[8] F. Farassat and M.K. Myers. A study of wave propagation in a duct and mode radiation. *2nd AIAA/CEAS Aeroacoustic Conference* AIAA paper 96-1677 (1996).

[9] S. T. Hocter. Exact and approximate directivity patterns of the sound radiated from a cylindrical duct. *Journal of Sound and Vibration* 227(2) (1999) 397-407.

[10] S. T. Hocter. Sound radiated from a cylindrical duct with Keller's geometrical theory. *Journal of Sound and Vibration* 231(5) (2000) 1243-1256.

[11] G.F. Homicz and J.A. Lordi. A note on the radiative directivity patterns of duct acoustics modes. *Journal of Sound and Vibration* 41(3) (1975) 283-290.

[12] U. Ingard and V.K. Singhal. Effect of flow on the acoustic resonances of an open-ended duct. *Journal of the Acoustical Society of America* 58(4) (1975) 788-793.

[13] P. Joseph and C. L. Morfey. Multimode radiation from an unflanged, semi-infinite circular duct. *Journal of the Acoustical Society of America* 105(5) (1999) 2590-2600.

[14] P. Joseph, P.A. Nelson and M.J. Fisher. Active Control of fan tones radiated from turbofan engines. I. External error sensors. *Journal of the Acoustical Society of America* 106(2) (1999) 766-778.

[15] G.W. Johnson an K. Ogimoto. Sound radiation from a finite length unflanged circular duct with uniform axial flow. I. Theoretical analysis. II. Computed radiation. *Journal of the Acoustical Society of America* 66(6) (1980) 1858-1870 (part I), 1871-1883 (part II).

[16] G.M. Keith. A theoretical investigation into the acoustic radiation from an aeroengine intake. *PhD Thesis, University of Cambridge* (2000).

[17] P.M. Morse and U. Ingard. *Theoretical Acoustics* McGraw Hill Books Company (1968).

[18] C. L. Morfey. Sound transmission and generation in ducts with flows. *Journal of Sound and Vibration* 14(1) (1971) 37-55.

[19] R. M. Munt. Acoustic transmission properties of a jet pipe with subsonic jet flow : I. the cold jet reflection coefficient. *Journal of Sound and Vibration* 142(3) (1990) 413-436.

[20] S. W. Rienstra. Acoustic radiation from a semi-infinite annular duct in a uniform subsonic mean flow. *Journal of Sound and Vibration* 42(3) (1975) 363-386.

[21] S. D. Savkar. Radiation of cylindrical duct acoustics modes with flow mismatch. *Journal of Sound and Vibration* 42(3) (1975) 363-386.

[22] J.M. Tyler and T.G. Sofrin. Axial compressor noise studies. *SAE Transactions* 70 (1962).

[23] F. Vanel-Hutcheson. Advanced modeling of active control of fan noise for ultra high bypass turbofan engine. *PhD Thesis, Virginia Polytechnic Institute and State University* (1999).

[24] M. Willatzen. Sound propagation in a moving fluid confined by cylindrical walls - Exact series representation for radially dependent flow profiles. *acta acustica - ACUSTICA* 87 (2001) 552-559..

A Green's function of a jet

The result presented in this appendix is classical and is intended to facilitate the reading of the text. Let us consider an infinite domain with a cylindrical reference coordinate (see figure 2) (O, r, θ, z). A fluid, with density ρ_e and sound wave celerity c_e occupies part of this domain. The fluid flow velocity is uniform with speed U_e parallel to the z axis. At the origin an an infinitely long cylindrical domain with radius a, contains a fluid with density ρ_i and sound wave celerity c_i and moves with uniform movement at speed U_i. The pressure and displacement are assumed to be contuinuous. The time dependence is also supposed to be harmonic $\exp(-\imath\omega t)$.

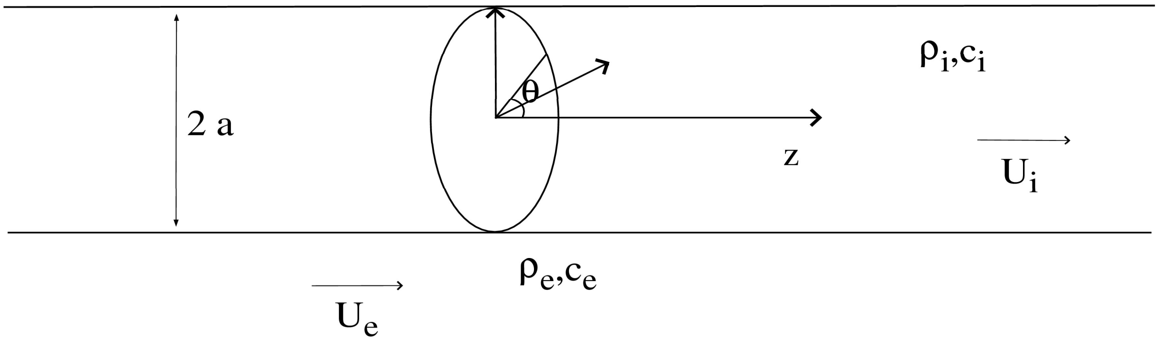

Figure 2: Geometry of the jet

Because of the 2π-periodicity of the geometry, all quantities have been expanded into angular Fourier series. One has:

$$f(r,\theta,z,t) = \sum_{m=-\infty}^{m=+\infty} f_m(r,z)\mathrm{e}^{\imath m\theta}\mathrm{e}^{-\imath\omega t}.$$

For each angular harmonic m, the Green's function $G_m(r,z;r_0,z_0)$ is the solution of

$$\begin{aligned}
\left(\frac{1}{r}\frac{\partial}{\partial r}r\frac{\partial}{\partial r} + \frac{m^2}{r^2} - \frac{1}{c_i^2}\left(-\imath\omega + U_i\frac{\partial}{\partial z}\right)^2 + \frac{\partial^2}{\partial z^2}\right)G_m(r,z;r_0,z_0) &= \frac{\delta(r-r_0)}{r}\delta(z-z_0), \text{ for } r<a \\
\left(\frac{1}{r}\frac{\partial}{\partial r}r\frac{\partial}{\partial r} + \frac{m^2}{r^2} - \frac{1}{c_e^2}\left(-\imath\omega + U_e\frac{\partial}{\partial z}\right)^2 + \frac{\partial^2}{\partial z^2}\right)G_m(r,z;r_0,z_0) &= 0, \text{ for } r \geq a.
\end{aligned}$$

$G_m(r,z;r_0,z_0)$ is calculated by Fourier transform with respect to z

$$\tilde{G}_m(r,k_z;r_0,z_0) = \int_{-\infty}^{+\infty} G_m(r,z;r_0,z_0)\mathrm{e}^{-\imath k_z z}\mathrm{d}z.$$

then

$$\begin{aligned}
\left(\frac{1}{r}\frac{\partial}{\partial r}r\frac{\partial}{\partial r} + \frac{m^2}{r^2} + \kappa_i^2\right)\tilde{G}_m(r,k_z;r_0,z_0) &= \frac{\delta(r-r_0)}{r}\mathrm{e}^{-\imath k_z z_0}, \text{ for } r<a \\
\left(\frac{1}{r}\frac{\partial}{\partial r}r\frac{\partial}{\partial r} + \frac{m^2}{r^2} + \kappa_e^2\right)\tilde{G}_m(r,k_z;r_0,z_0) &= 0, \text{ for } r \geq a,
\end{aligned}$$

where $\kappa_i^2 = (k_0^i + M_i k_z)^2 - k_z^2$ and $\kappa_e^2 = (k_0^e + M_e k_z)^2 - k_z^2$, with $k_0^{i,e} = \omega/c_{i,e}$ and $\Im(\kappa_{i,e}) > 0$.

The solution of $(1/r\partial_r r\partial_r + m^2/r^2 + \kappa_i^2)\,\tilde{G}_m(r;r_0) = \delta(r-r_0)/r$ is given by ([17], p. 366)

$$\begin{aligned}\tilde{G}_m(r,k_z;r_0,z_0) &= -\frac{\imath\pi}{2}\mathrm{H}_m(\kappa_i r_0)\mathrm{J}_m(\kappa_i r), r < r_0\\ \tilde{G}_m(r,k_z;r_0,z_0) &= -\frac{\imath\pi}{2}\mathrm{H}_m(\kappa_i r)\mathrm{J}_m(\kappa_i r_0), r \geq r_0\end{aligned}$$

where $\mathrm{H}_m(z)$ is the Hankel function of the first kind. The interface at $r = a$ involves the presence of a reflected field $\tilde{G}_{Rm}(r;r_0)$ and a transmitted one $\tilde{G}_{Tm}(r;r_0)$. One has:

$$\begin{aligned}\tilde{G}_{Rm}(r;r_0) &= -\frac{\imath\pi}{2}\mathrm{J}_m(\kappa_i r_0)R_m(k_z)\mathrm{J}_m(\kappa_i r)\\ \tilde{G}_{Tm}(r;r_0) &= -\frac{\imath\pi}{2}\mathrm{J}_m(\kappa_i r_0)T_m(k_z)\mathrm{H}_m(\kappa_e r),\end{aligned}$$

where $R_m(k_z)$ and $T_m(k_z)$ are reflection and transmission coefficients. These coefficients are calculated by imposing the continuity conditions. One obtains:

$$\begin{aligned}\mathrm{H}_m(\kappa_i a) + \mathrm{J}_m(\kappa_i a)R_m(k_z) &= \mathrm{H}_m(\kappa_e a)T_m(k_z).\\ \mathrm{H}'_m(\kappa_i a) + \mathrm{J}'_m(\kappa_i a)R_m(k_z) &= \alpha_m(k_z)\mathrm{H}'_m(\kappa_e a)T_m(k_z), \alpha_m(k_z) = \frac{\kappa_e\rho_i(\omega + U_i k_z)^2}{\kappa_i\rho_e(\omega + U_e k_z)^2}.\end{aligned}$$

Combining these relations gives the transmission coefficient:

$$T_m(k_z) = -\frac{2\imath}{\pi\kappa_i a}\frac{1}{\mathrm{J}'_m(\kappa_i a)\mathrm{H}_m(\kappa_e a) - \alpha_m(k_z)\mathrm{H}'_m(\kappa_e a)\mathrm{J}_m(\kappa_i a)}.$$

Then finally, by inverse Fourier transform

$$G_m(r,z;r_0,z_0) = -\frac{\imath}{4}\int_{-\infty}^{+\infty}\mathrm{J}_m(\kappa_i r_0)\mathrm{H}_m(\kappa_e r)T_m(k_z)\mathrm{e}^{\imath k_z(z-z_0)}\mathrm{d}k_z, r \geq a$$

Bonjour

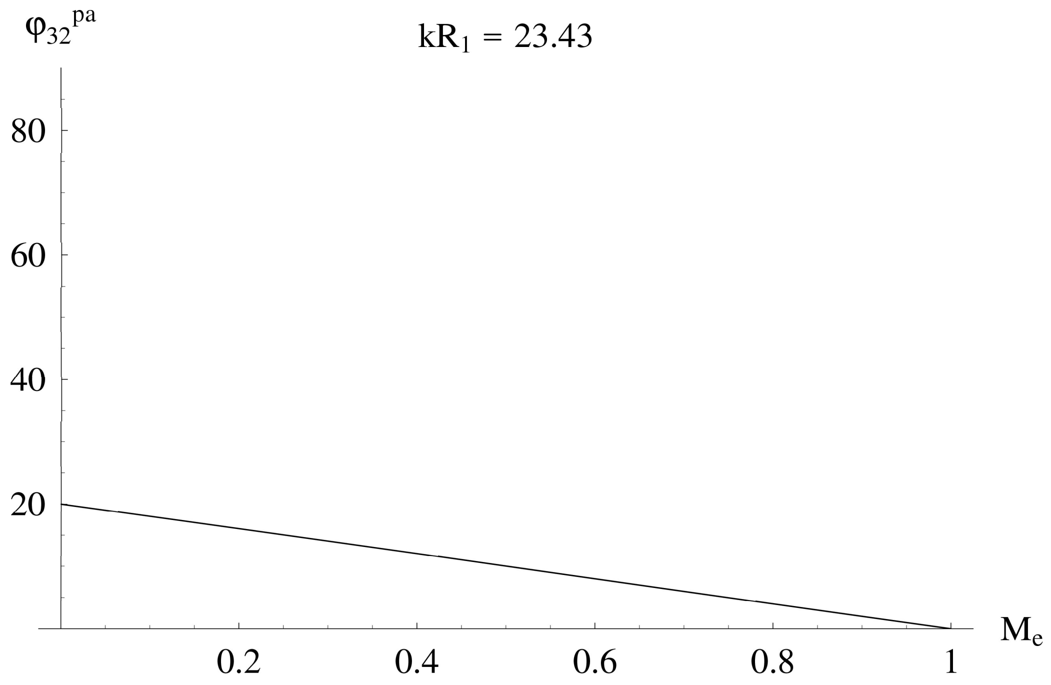

Figure 3: Change of the upstream maximum directivity of the (3,2) mode with the external Mach number

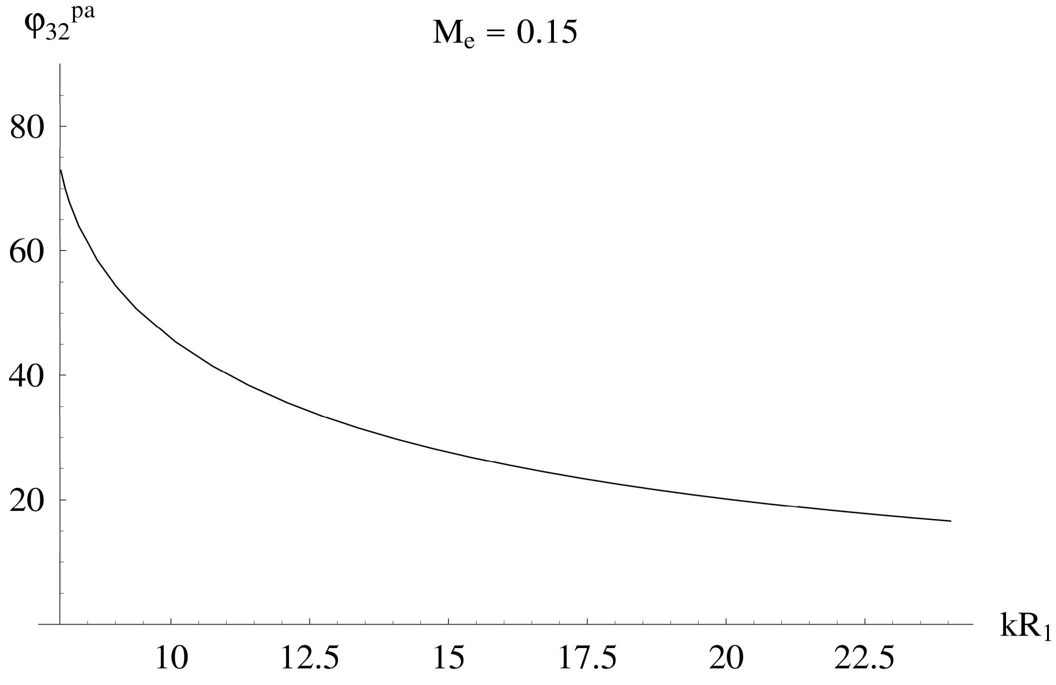

Figure 4: Change of the upstream maximum directivity of the (3,2) mode with the frequency

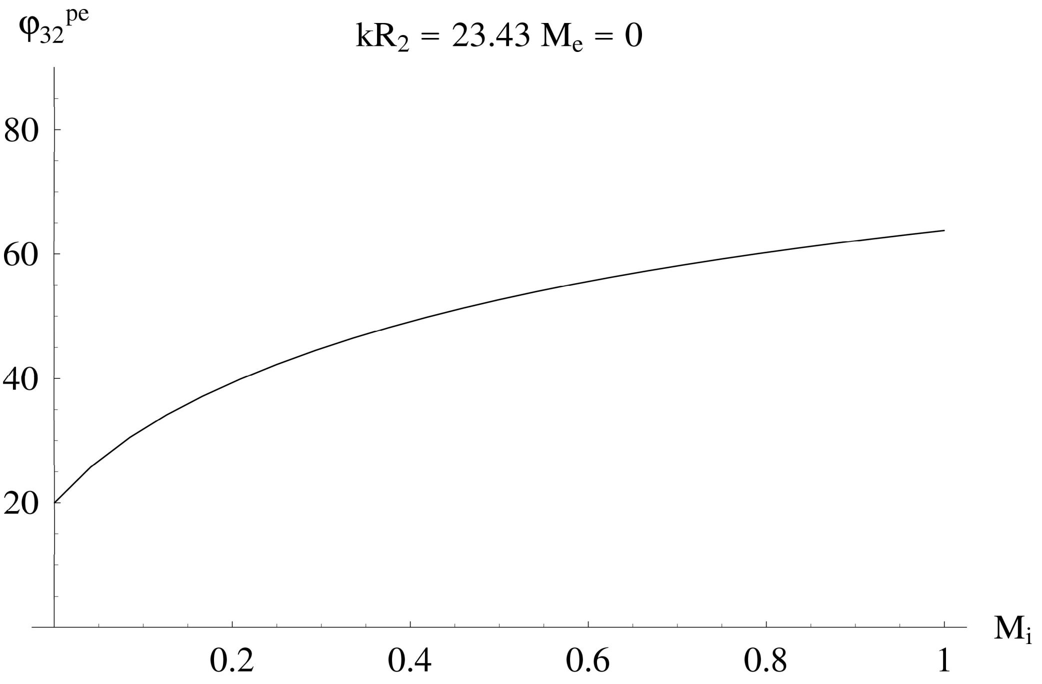

Figure 5: Change of the downstream maximum directivity of the (3,2) mode with the internal Mach number

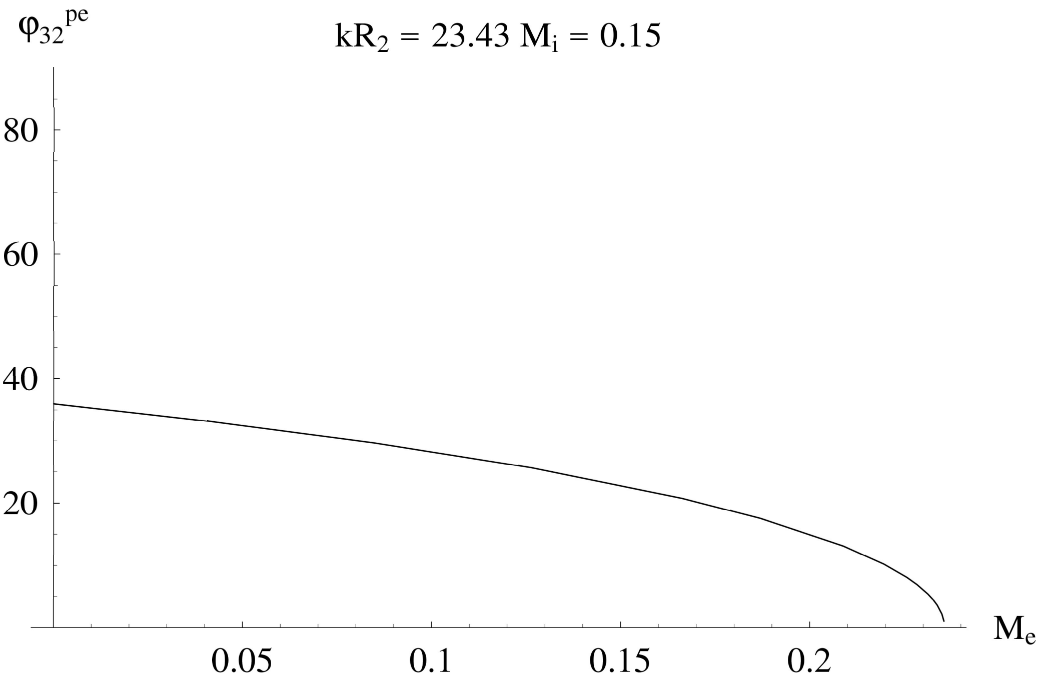

Figure 6: Change of the downstream maximum directivity of the (3,2) mode with the external Mach number

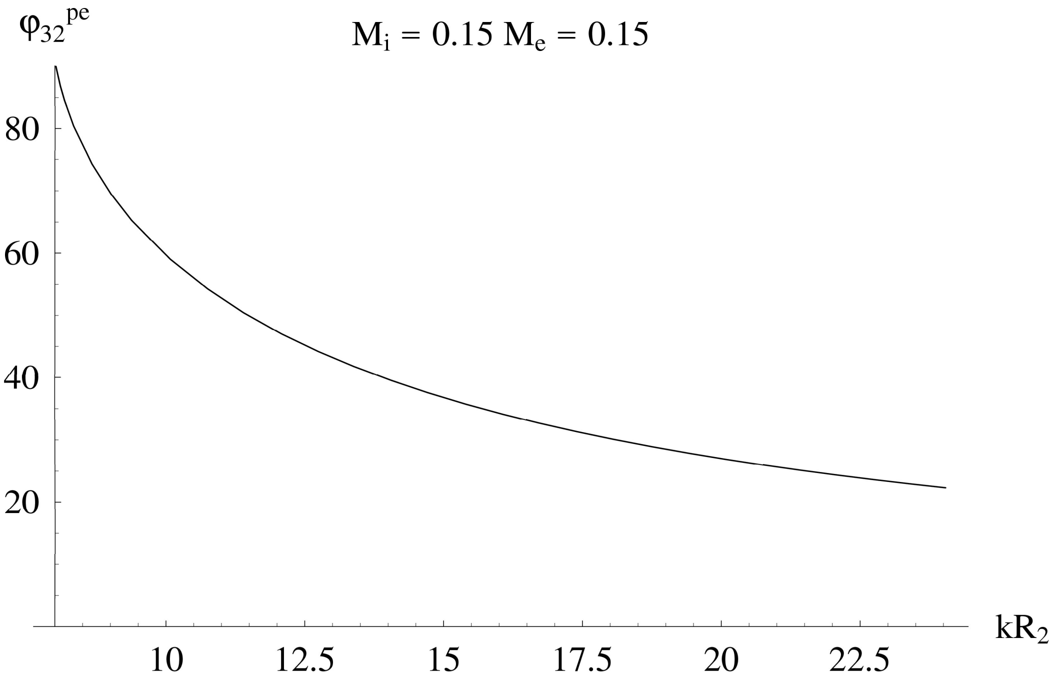

Figure 7: Change of the downstream maximum directivity of the (3,2) mode with the frequency

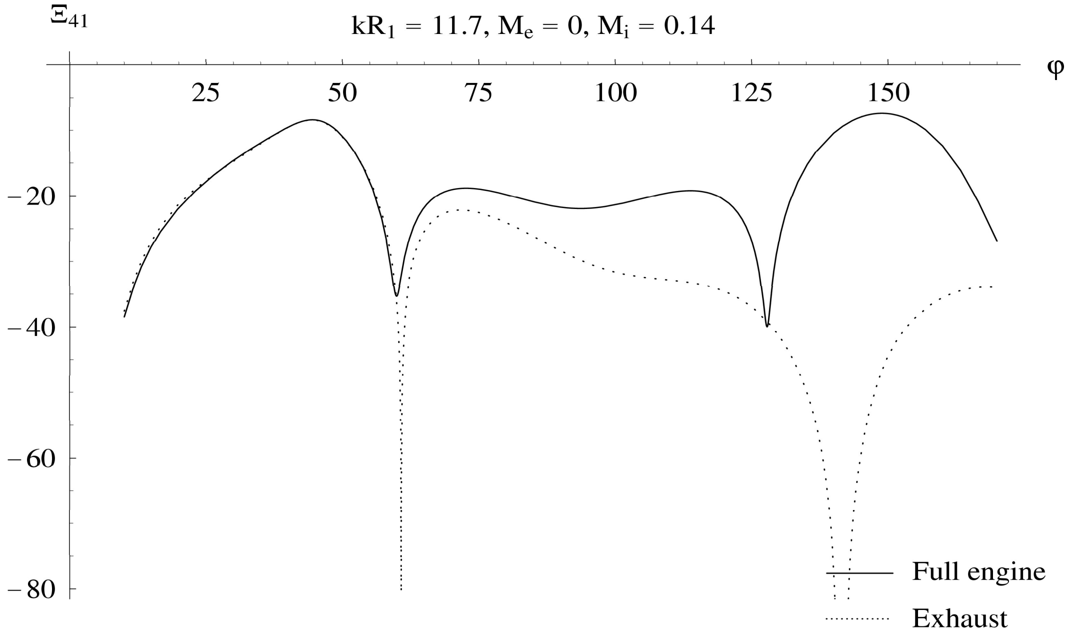

Figure 8: Comparison betwwen the directivities of the exhaust alone and that of the aeroengine at rest for the (4,1) mode

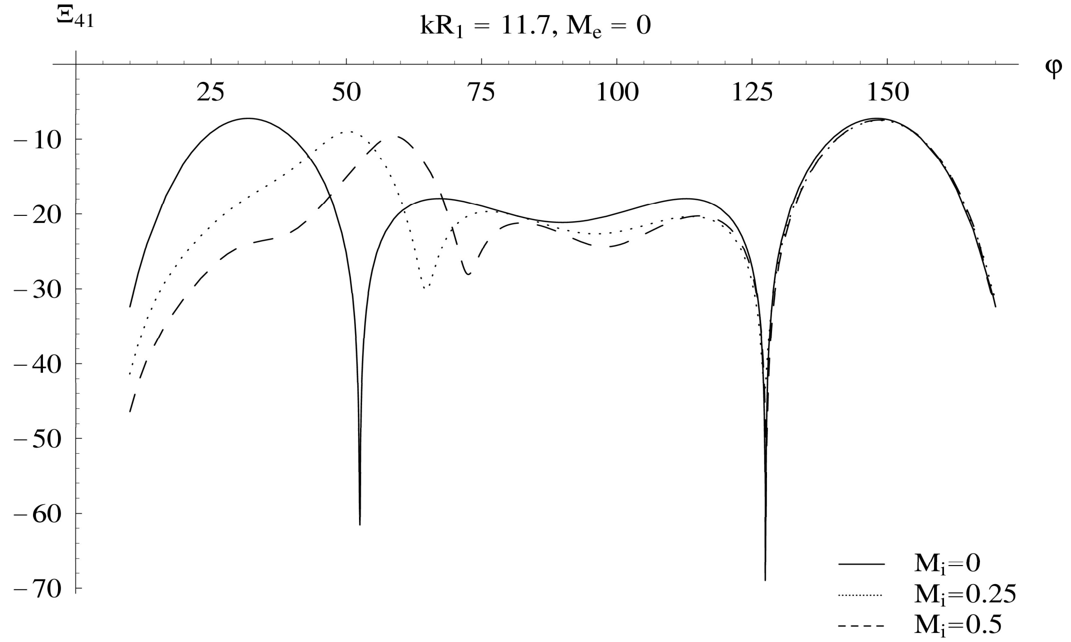

Figure 9: Influence of the jet Mach number on the directivity of the aeroengine at rest for the (4,1) mode

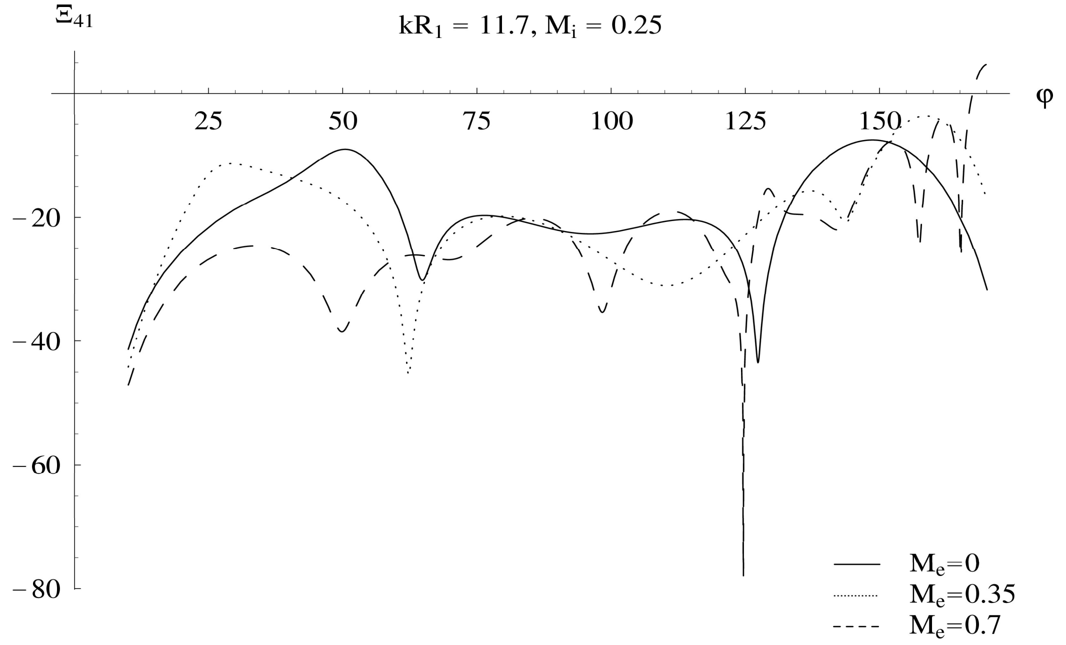

Figure 10: Influence of the external Mach number on the directivity of the moving aeroengine for the (4,1) mode

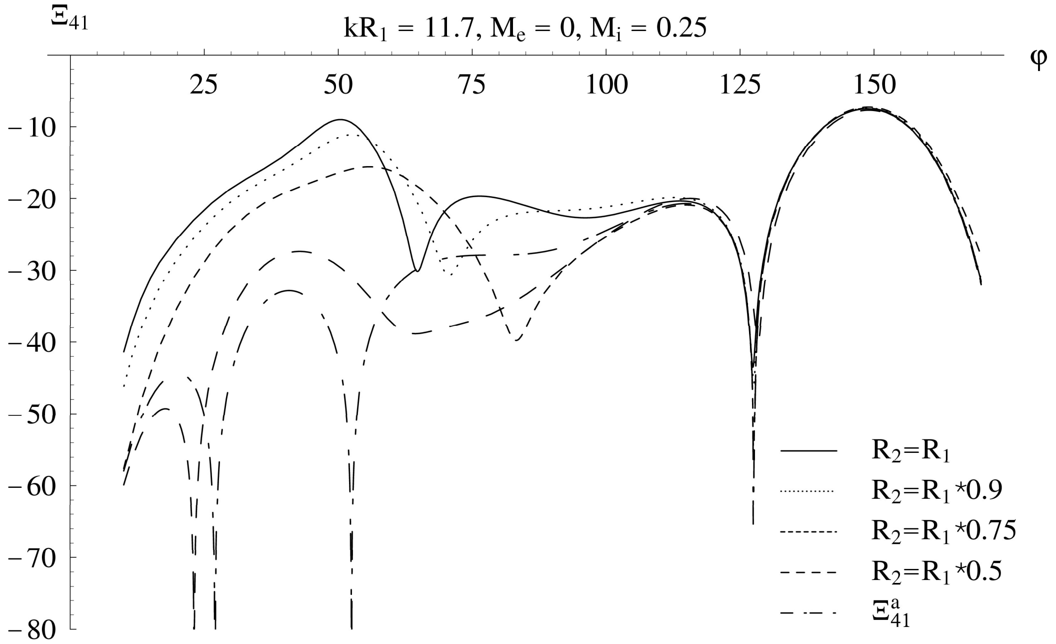

Figure 11: Influence of the exhaust radius on the directivity of the aeroengine at rest for the (4,1) mode

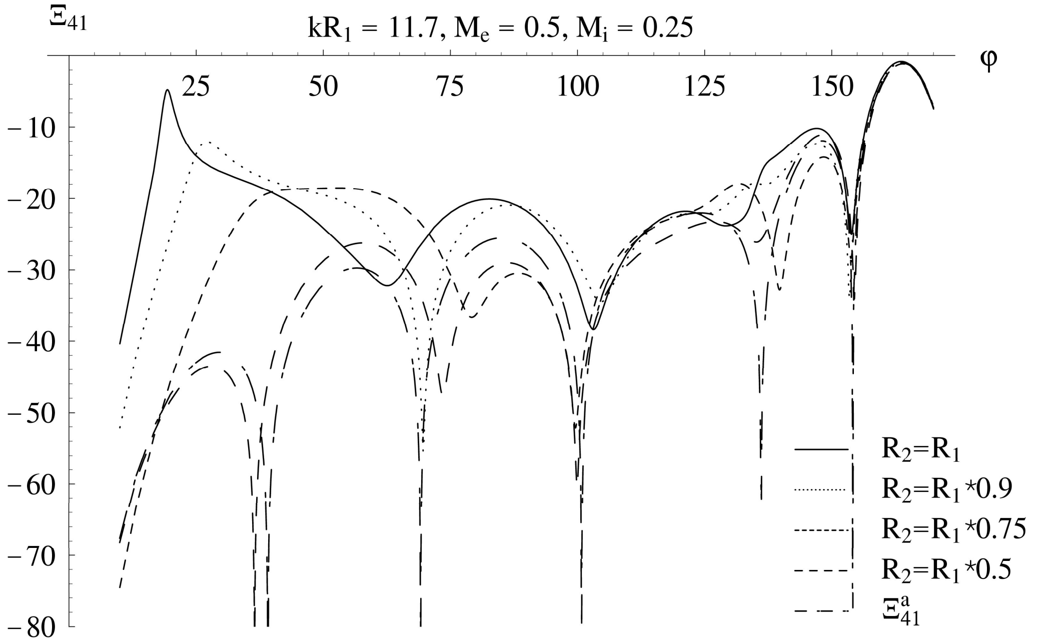

Figure 12: Influence of the radius of the exhaust on the directivity of the aeroengine for the (4,1) mode

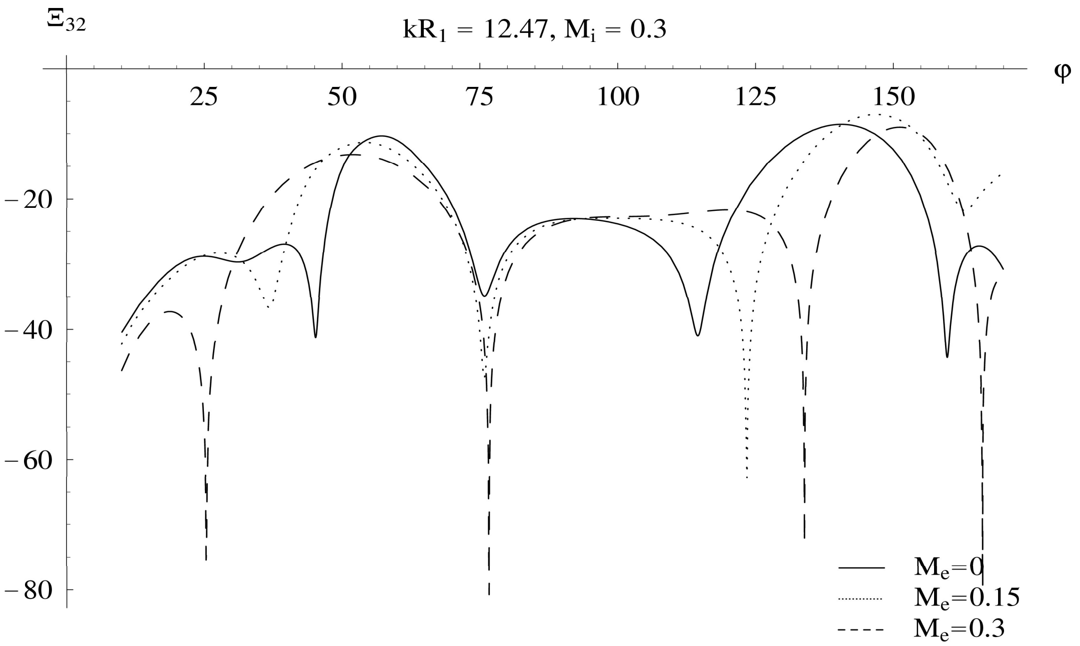

Figure 13: Influence of the external Mach number on the directivity of the aeroengine at low jet Mach numbers for the (3,2) mode

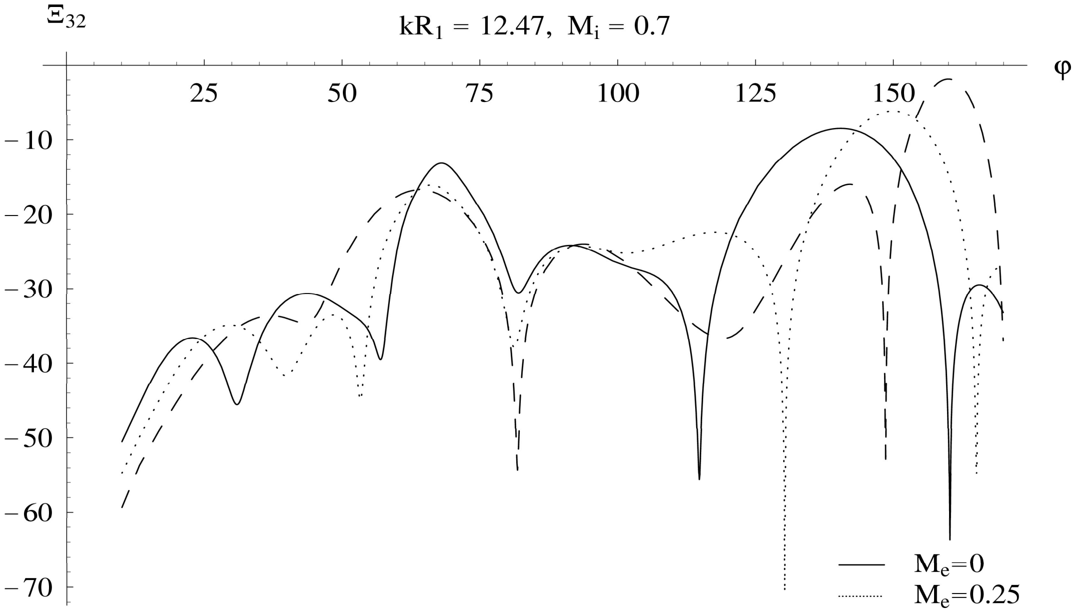

Figure 14: Influence of the external Mach number on the directivity of the aeroengine at high jet Mach numbers for the (3,2) mode

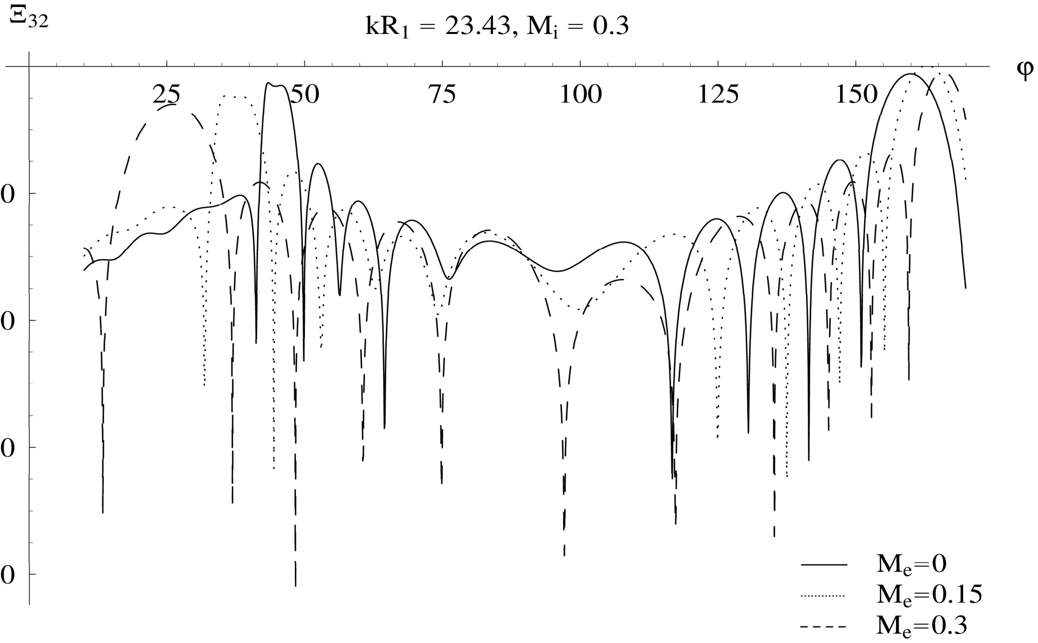

Figure 15: Influence of the external Mach number on the high frequency directivity of the aeroengine at low jet Mach number for the (3,2) mode

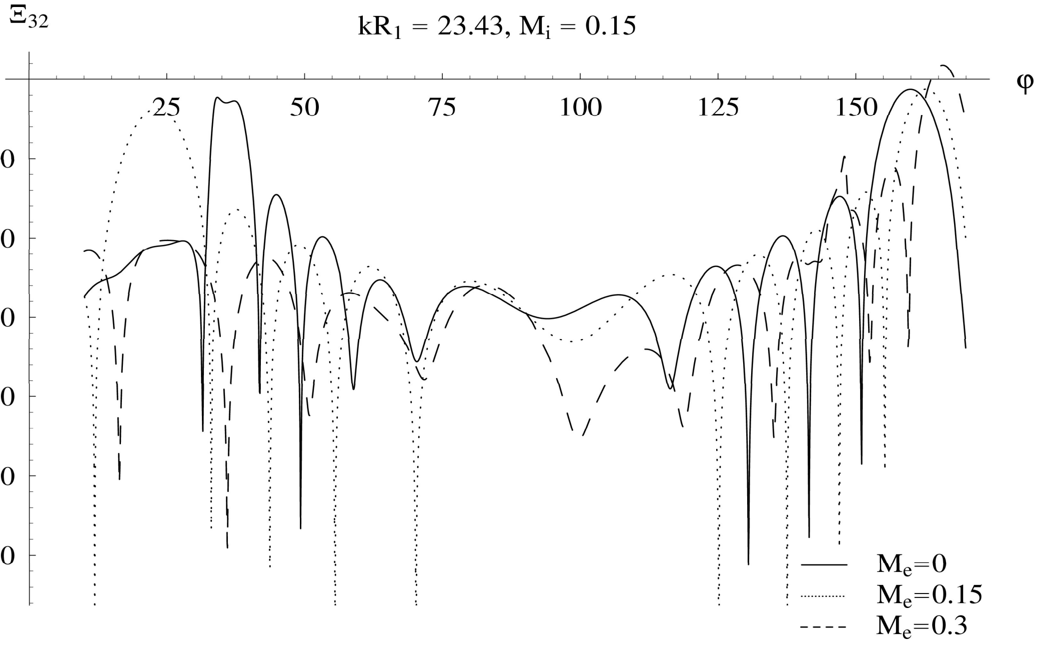

Figure 16: Influence of the external Mach number on the high frequency directivity of the moving aeroengine at very low jet Mach numbers for the (3,2) mode